

Studies on Magnetic Susceptibility, Electron Paramagnetic Resonance, and Absorption Spectrum of Li_3UO_4 , an Octahedral U^{5+} Compound with a Small Tetragonal Distortion

YUKIO HINATSU AND TAKEO FUJINO*

*Department of Chemistry, Japan Atomic Energy Research Institute,
Tokai-mura, Ibaraki 319-11, Japan*

AND NORMAN EDELSTEIN

*Materials and Chemical Sciences Division, Lawrence Berkeley Laboratory,
University of California, Berkeley, California 94720*

Received August 22, 1991; in revised form January 2, 1992; accepted January 7, 1992

Li_3UO_4 was prepared, and its magnetic susceptibility was measured from 4.2 K to room temperature. The electron paramagnetic resonance signal was not detected even at 4.2 K. The magnetic susceptibility and the absorption spectrum were analyzed on the basis of an octahedral crystal field model with a small tetragonal distortion. Calculated anisotropic g -values and the magnetic susceptibility were also compared with the experimental results reported previously. © 1992 Academic Press, Inc.

Introduction

It is well known that the $5f$ electrons which characterize the magnetic and optical properties of actinides are not so well localized as the $4f$ electrons in the rare earths, and that for the $5f$ compounds, the crystal-field interaction is a larger perturbation on the spin-orbit coupling interaction than that for the $4f$ compounds. In many cases, the crystal field, spin-orbit coupling, and electronic repulsion interactions are of comparable magnitude, which makes the analysis of the experimental results complicated. However, for the actinide ions having the

$[\text{Rn}]5f^1$ electronic configuration as in the case of U^{5+} , the situation is considerably simplified, because there is no electron-electron repulsion interaction.

For the single $5f$ electron in an octahedral coordination, several theoretical studies have been reported on the crystal-field interactions including the effect of covalent bonding (1–4). Selbin *et al.* (5) extended the theory for a single $5f$ electron in octahedral crystal-field symmetry to the tetragonally distorted system. Kanellakopoulos *et al.* (6) measured optical spectra and magnetic susceptibilities for a number of uranates (U^{5+}), neptunates (Np^{6+}), and one plutonate (Pu^{7+}), and fitted their data to the theory developed by Selbin *et al.* However, an added empirical temperature-independent paramagnetic susceptibility was

* Present address: Research Institute of Mineral Dressing and Metallurgy, Tohoku University, Sendai 980, Japan.

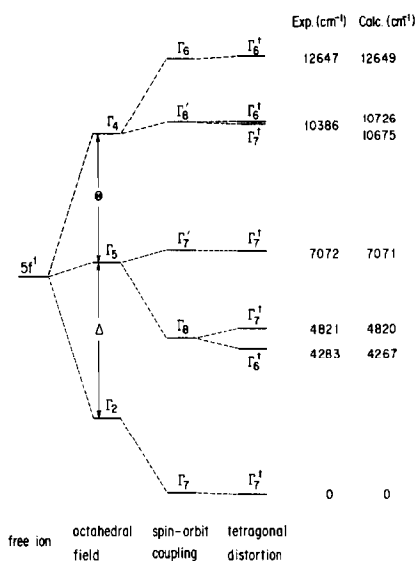


FIG. 1. f^1 orbital splitting perturbed by octahedral crystal field, spin-orbit coupling, and tetragonal distortion.

needed to obtain a satisfactory fit of the magnetic susceptibility data as a function of temperature.

We focus attention in this paper on the optical and magnetic properties of Li_3UO_4 . X-ray structure investigations indicate that this uranate is tetragonal and of the distorted NaCl type (7), that is, a central uranium ion is octahedrally coordinated by six oxygen ions and this oxygen octahedron shrinks along the fourfold rotation axis, changing the symmetry to tetragonal. Therefore, from the optical and magnetic study of Li_3UO_4 , we may obtain the effect of the tetragonal crystal field distortion on the electronic states of a $5f$ electron in octahedral coordination.

Kanellakopulos *et al.* (6) measured the optical spectra of Li_3UO_4 and reported that although the quartet Γ_8 state splits into two doublets the energy separation of which is 540 cm^{-1} , the splitting of higher energy quartet Γ_8' state is not observed, as shown schematically in Fig. 1. Magnetic suscepti-

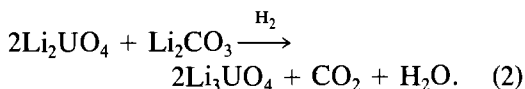
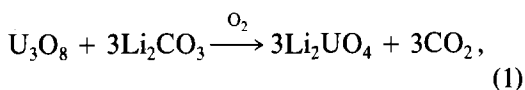
bilities and electron paramagnetic resonance (EPR) spectra were measured by several groups. However, the results were not consistent. Kemmler-Sack *et al.* (8) measured the magnetic susceptibility of Li_3UO_4 from 83 to 473 K and found that it did not obey the Curie-Weiss law but could be represented by $\chi = 0.045/T + 290 \times 10^{-6}$ (emu/mole). Keller (9) extended the temperature range of the magnetic susceptibility measurements of Li_3UO_4 down to 4.2 K and found a large field dependence of the magnetic susceptibility below 7 K. Kanellakopulos *et al.* (6) made detailed measurements of the temperature and field dependence of the magnetic susceptibility of Li_3UO_4 and obtained results quite similar to those reported by Keller. Miyake *et al.* (10) also measured the field dependence of the magnetic susceptibility at 4.2 K. Lewis *et al.* (11) reported that they could not observe any EPR spectrum for Li_3UO_4 even at 4.2 K. On the contrary, Miyake *et al.* (10) measured a broad EPR spectrum at room temperature and 77 K and found a g -value of 2.35–2.50.

In order to clarify the inconsistent experimental results and to elucidate the behavior of the $5f$ electron in an octahedral crystal field with a small tetragonal distortion, we prepared Li_3UO_4 , and carried out magnetic susceptibility measurements in the temperature range of 4.2 K to room temperature and EPR measurements at 4.2 K. The crystal-field parameters were obtained from the analysis of the optical absorption spectrum. The magnetic susceptibility was calculated and compared with the experimental data. From this we derive the anisotropic g -values and discuss the reported experimental data.

Experimental

1. Preparation

Li_3UO_4 was prepared by the following reactions:



Li_2UO_4 was prepared by repeatedly grinding and firing to 850°C mixtures of U_3O_8 and Li_2CO_3 in air for 1 day. Li_3UO_4 was prepared by heating mixtures of Li_2UO_4 and Li_2CO_3 in a flow of hydrogen gas at 800°C for 10 hr. After cooling to room temperature, the sample was crushed into powder, pressed into pellets, and reduced under the same conditions.

2. Analysis

2.1. X-ray diffraction analysis. An X-ray diffraction study was performed with $\text{CuK}\alpha$ radiation on a Philips PW 1390 diffractometer equipped with a curved graphite monochromator. The lattice parameters of the samples were determined by a least-squares method applied to the diffraction lines.

2.2. Determination of oxygen amount. The oxygen nonstoichiometry in the specimen was checked by the back-titration method (12, 13). A weighed sample was dissolved in excess cerium (IV) sulfate solution. The cerium (IV) sulfate solution was standardized in advance with stoichiometric UO_2 . The excess cerium (IV) was titrated against a standard iron (II) ammonium sulfate solution with ferroin indicator. The oxygen amount was determined for predetermined Li/U ratio.

3. Magnetic Susceptibility Measurement

The magnetic susceptibility was measured with a Faraday-type torsion balance in the temperature range of 4.2 K to room temperature. The apparatus was calibrated with a Manganese Tutton's salt ($\chi_g = 10980 \times 10^{-6}/(T + 0.7)$) standard. The temperature of the sample was measured

by a "normal" Ag vs Au-0.07 at% Fe thermocouple (4.2 ~ 40 K) (14) and an Au-Co vs Cu thermocouple (10 K ~ room temperature). Details of the experimental procedure have been described elsewhere (15).

4. Electron Paramagnetic Resonance Measurement

The EPR measurements were carried out both at room temperature and at 4.2 K for the specimen sealed in a quartz tube. The measurements were made using a JEOL 2XG spectrometer operating at 9.10 GHz with 100 kHz field modulation. The magnetic field was swept from 100 to 12,000 G. Before measuring the specimen, a blank was recorded to eliminate the possibility of interference by the background resonance of the cavity and/or sample tube.

Results

The X-ray diffraction analysis shows the specimen is tetragonal and the lattice parameters are $a = 4.484 \text{ \AA}$ and $c = 8.479 \text{ \AA}$. From the chemical analysis of the oxygen concentration, the specimen prepared in this study was found to be oxygen stoichiometric, $\text{Li}_3\text{UO}_{4.008}$.

The temperature dependence of the reciprocal magnetic susceptibility is shown in Fig. 2. In this figure, the susceptibility data measured by other research groups are also drawn. Our susceptibility data are close to those of Kanellakopulos *et al.*, but discrepancies between the data become greater in the lower temperature region. Figure 3 shows the dependence of magnetic susceptibility on field strength at 4.2, 77.3, and 298 K. Clearly, a field dependence of the magnetic susceptibility was found at 4.2 K. Kanellakopulos *et al.* also found a similar field dependence of the magnetic

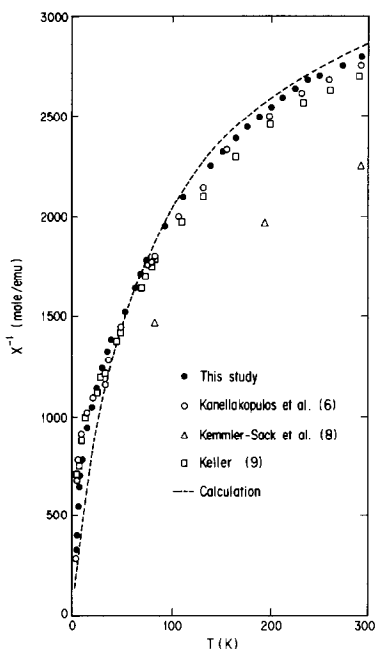


FIG. 2. Reciprocal magnetic susceptibilities versus temperature.

susceptibility at 4.2 K, which is depicted in the same figure.

No EPR signal was observed even at 4.2 K. This result is consistent with the result by Lewis *et al.* (11), but different from the result by Miyake *et al.* (10).

Discussion

The crystal structure of Li_3UO_4 is tetragonal and of the distorted NaCl type with the central uranium ion octahedrally coordinated by six oxygen ions. This oxygen octahedron shrinks along the fourfold rotation axis (7). The optical spectrum indicates that Li_3UO_4 has a tetragonally distorted molecular symmetry.

Figure 1 shows the effects of perturbing the f^1 orbital energy levels successively by an octahedral crystal field, spin-orbit coupling, and tetragonal crystal-field distortion. In an octahedral crystal field, the sevenfold degen-

erate energy state of the f orbitals is split into Γ_2 , Γ_5 , and Γ_4 states, where Δ and Θ are parameters that represent the intensity of the crystal field. If spin-orbit coupling is taken into account, the Γ_2 orbital state is transformed into Γ_7 , whereas the Γ_5 and Γ_4 states are split into Γ_7^* and Γ_8 , and Γ_6 and Γ_8^* , respectively (16). The ground state Kramers doublet is the Γ_7 state and is coupled to the excited Γ_7^* state arising from the Γ_5 orbital, by spin-orbit coupling. The Γ_8 state arising from the Γ_5 orbital state is also coupled to the Γ_8^* state arising from the Γ_4 orbital state by the same spin-orbit coupling interaction. The energy matrices for the Γ_7 , Γ_8 , and Γ_6 states are

$$\begin{aligned} \Gamma_6: & \left| \Delta + \Theta + \frac{3}{2}\zeta \right|; \\ \Gamma_8: & \begin{vmatrix} \Delta + \frac{1}{4}\zeta & \frac{3}{4}\sqrt{5}\zeta \\ \frac{3}{4}\sqrt{5}\zeta & \Delta + \Theta - \frac{3}{2}\zeta \end{vmatrix}; \\ \Gamma_7: & \begin{vmatrix} 0 & \sqrt{3}\zeta \\ \sqrt{3}\zeta & \Delta - \frac{1}{2}\zeta \end{vmatrix}. \end{aligned} \quad (3)$$

Here ζ is the spin-orbit coupling constant. Diagonalization of the energy matrix produces the ground state Γ_7 and the excited state Γ_7^* , and the corresponding wavefunctions are written as

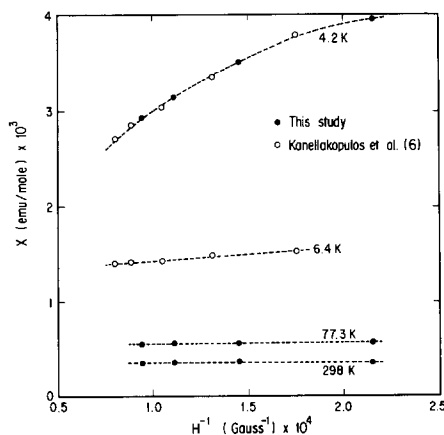


FIG. 3. Field dependence of magnetic susceptibilities.

$$\begin{aligned} |\Gamma_7\rangle &= \cos \theta |^2F_{5/2}, \Gamma_7\rangle - \sin \theta |^2F_{7/2}, \Gamma_7^*\rangle \\ |\Gamma_7'\rangle &= \sin \theta |^2F_{5/2}, \Gamma_7\rangle + \cos \theta |^2F_{7/2}, \Gamma_7^*\rangle, \end{aligned} \quad (4)$$

where θ is the parameter describing the admixture of the Γ_7 levels in the ground state. Similarly, diagonalization of the Γ_8 matrix produces the two levels Γ_8 and Γ_8' .

The effect of the tetragonal distortion is that the ground state Γ_7 is transformed into Γ_7^1 , whereas the excited states are split or transformed according to $\Gamma_8 \rightarrow \Gamma_8^1 + \Gamma_8^1$, $\Gamma_7' \rightarrow \Gamma_7^1$, $\Gamma_8' \rightarrow \Gamma_8^1 + \Gamma_8^1$, and $\Gamma_6 \rightarrow \Gamma_6^1$ (Fig. 1). Also this effect introduces three additional

terms into the Hamiltonian in addition to the octahedral terms,

$$V_{\text{tet}} = \tau V_2^0 + \gamma V_4^0 + \delta V_6^0. \quad (5)$$

Here τ , γ , and δ are parameters which depend on the radial functions, and V_2^0 , V_4^0 , and V_6^0 transform like the spherical harmonics of order 2, 4, and 6, respectively. To reduce the number of parameters, and since the τV_2^0 term is expected to be dominant, we will take only this term into account, as do Selbin *et al.* (5) and Kanellakopoulos *et al.* (6). The complete energy matrices for the tetragonal Γ_7 and Γ_6 , and the corresponding wavefunctions are as follows:

$$\Gamma_7: \begin{vmatrix} \Gamma_7^1 & \Gamma_7^{*1} & \Gamma_8^1 & \Gamma_8^{*1} \\ \Gamma_7^2 & \Gamma_7^{*2} & \Gamma_8^2 & \Gamma_8^{*2} \\ 0 & \sqrt{3}\zeta & 0 & 0 \\ \sqrt{3}\zeta & \Delta - \frac{1}{2}\zeta & 0 & \sqrt{10}\tau \\ 0 & 0 & \Delta + \frac{1}{4}\zeta & \frac{3}{4}\sqrt{5}\zeta + \sqrt{5}\tau \\ 0 & \sqrt{10}\tau & \frac{3}{4}\sqrt{5}\zeta + \sqrt{5}\tau & \Delta + \Theta - \frac{3}{4}\zeta - 2\tau \end{vmatrix} \quad (6)$$

$$\Gamma_6: \begin{vmatrix} \Gamma_8^3 & \Gamma_8^{*3} & \Gamma_6^1 \\ \Gamma_8^4 & \Gamma_8^{*4} & \Gamma_6^2 \\ \frac{\Delta + \frac{1}{4}\zeta}{\sqrt{10}\tau} & \frac{\frac{3}{4}\sqrt{5}\zeta - \sqrt{5}\tau}{2\sqrt{2}\tau} & \frac{\sqrt{10}\tau}{2\sqrt{2}\tau} \\ \frac{\frac{3}{4}\sqrt{5}\zeta - \sqrt{5}\tau}{\sqrt{10}\tau} & \Delta + \Theta - \frac{3}{4}\zeta + 2\tau & \Delta + \Theta + \frac{3}{2}\zeta \end{vmatrix}. \quad (7)$$

From the optical absorption spectra measured by Kanellakopoulos *et al.*, we determined the ligand field parameters Δ and Θ , the spin-orbit coupling constant ζ , and the tetragonal distortion parameter τ . Since the splitting of the Γ_8' level is not experimentally observed, the degree of tetragonal distortion is considered to be fairly small. Thus we first approximately determine Δ , Θ , and ζ by assuming octahedral symmetry around the central uranium ion. By fitting the transition energies experimentally obtained to those calculated by solving Eq. (3), we obtained $\Delta = 4517 \text{ cm}^{-1}$, $\Theta = 3713 \text{ cm}^{-1}$, and $\zeta =$

1750 cm^{-1} . Next, we took into account the tetragonal distortion effect, which resulted in the splitting of both quartets Γ_8 and Γ_8' into two Kramers doublets. The experimental results from the optical absorption spectrum show that the Γ_8 splits into Γ_8^1 and Γ_8^1 , the energy difference between these states is 540 cm^{-1} , whereas the splitting of Γ_8' is not observed (6). By diagonalizing energy matrices, Eqs. (6) and (7), we obtained the energies for each level. For six transition energies, the parameters Δ , Θ , ζ , and τ were adjusted, i.e., the remaining two transitions were used as a criterion for the

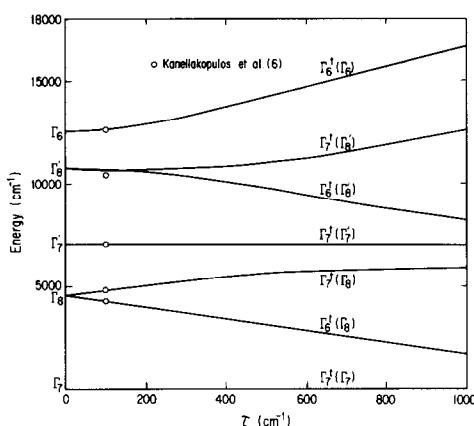


FIG. 4. The splitting of the $5f$ manifold of octahedral energy levels with increasing tetragonal distortion.

calculation to get better values for the crystal-field parameters and the spin-orbit coupling constant. Unfortunately, not all the transitions were fitted. Since the transition $\Gamma_7 \rightarrow \Gamma_8'$ for octahedral symmetry is known to be broad and since this transition is furthermore broadened due to the tetragonal distortion, we have considered the $\Gamma_7 \rightarrow \Gamma_8'$ transition energy to be the least reliable. We obtained $\Delta = 4517 \text{ cm}^{-1}$, $\Theta = 3693 \text{ cm}^{-1}$, $\zeta = 1750 \text{ cm}^{-1}$, and $\tau = 100 \text{ cm}^{-1}$. The spin-orbit coupling constant obtained here is considered to be an acceptable value for U^{5+} in solids (17). This magnitude of the spin-orbit coupling constant has been obtained also by others (5, 6, 18–20) and the magnitude is intermediate between those of Pa^{4+} and Np^{6+} compounds (21).

Figure 4 shows the splitting of the octahedral energy levels with increasing tetragonal distortion τ . This figure indicates that [1] the $\Gamma_7 \rightarrow \Gamma_7'$ transition is nearly unaltered, [2] the Γ_8 and Γ_8' levels are significantly split, and [3] the Γ_6 energy is greatly increased. However, the situation is a little different for a small tetragonal distortion ($\tau < 150 \text{ cm}^{-1}$). The splitting of Γ_8' into Γ_6' and Γ_7' levels is negligibly small compared with the large splitting of Γ_8 . The energy increase of

the Γ_6 level is small. For $\tau = 100 \text{ cm}^{-1}$, the transition energies calculated for $\Gamma_7^1(\Gamma_7) \rightarrow \Gamma_6^1(\Gamma_8)$, $\Gamma_7^1(\Gamma_7) \rightarrow \Gamma_7^1(\Gamma_8)$, $\Gamma_7^1(\Gamma_7) \rightarrow \Gamma_7^1(\Gamma_7')$, and $\Gamma_7^1(\Gamma_7) \rightarrow \Gamma_6^1(\Gamma_6)$ are fitted very well to the experimental results. Although the transition energies calculated for $\Gamma_7^1(\Gamma_7) \rightarrow \Gamma_6^1(\Gamma_8')$ and $\Gamma_7^1(\Gamma_7) \rightarrow \Gamma_7^1(\Gamma_8')$ are a little higher than the experimental values, the calculated splitting of Γ_8' level is quite small and corresponds to the experimental results.

No EPR signal was observed for our Li_3UO_4 sample even at 4.2 K. The probable reason for this is the rapid spin-spin relaxation time. Lewis *et al.* (11) reported that although they could not detect any EPR signal for pure LiUO_3 , they successfully measured an EPR spectrum for LiUO_3 diluted with diamagnetic LiNbO_3 . We are planning to measure the EPR spectrum for the specimen of Li_3UO_4 diluted with diamagnetic compounds. Since the wavefunctions for the ground Γ_7 doublet are obtained by diagonalizing the energy matrix, Eq. (6), the g -value for this ground doublet can be easily estimated. They are written as follows:

$$\begin{aligned} |\Gamma_7\rangle &= C_1|\Gamma_7^1\rangle + C_2|\Gamma_7^{*1}\rangle + C_3|\Gamma_8^1\rangle + C_4|\Gamma_8^{*1}\rangle, \\ |\bar{\Gamma}_7\rangle &= C_1|\Gamma_7^2\rangle + C_2|\Gamma_7^{*2}\rangle + C_3|\Gamma_8^2\rangle + C_4|\Gamma_8^{*2}\rangle. \end{aligned} \quad (8)$$

Here $|\bar{\Gamma}_7\rangle$ is the Kramers conjugate wavefunction for the ground Γ_7 doublet. The g -values for this state are calculated by the following equations:

$$\begin{aligned} g_{\parallel} &= 2\langle\Gamma_7|L_z + 2S_z|\Gamma_7\rangle, \\ g_{\perp} &= 2\langle\Gamma_7|L_x + 2S_x|\bar{\Gamma}_7\rangle. \end{aligned} \quad (9)$$

So, the g_{\parallel} -value is calculated to be

$$\begin{aligned} g_{\parallel} &= 2(C_1^2 + \frac{1}{2}C_3^2 + \frac{1}{2}C_4^2 \\ &\quad + \frac{4}{\sqrt{3}}C_1C_2 + 4\sqrt{\frac{2}{3}}C_1C_3 + \sqrt{2}C_2C_3 \\ &\quad + \sqrt{10}C_2C_4 - \sqrt{5}C_3C_4). \end{aligned} \quad (10)$$

If we drop C_3^2 , C_4^2 , and C_3C_4 terms because of $C_3, C_4 \ll C_1, C_2$, g_{\parallel} is rewritten as

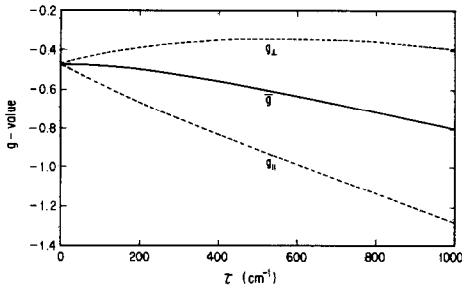


FIG. 5. The variation of g -value with tetragonal distortion.

$$g_{||} = 2(C_1^2 + \frac{4}{\sqrt{3}}C_1C_2) + 2\left(4\sqrt{\frac{2}{3}}C_1C_3 + \sqrt{2}C_2C_3 + \sqrt{10}C_2C_4\right), \quad (11)$$

$$= g_0 + 2\gamma,$$

where

$$g_0 = 2(C_1^2 + \frac{4}{\sqrt{3}}C_1C_2),$$

$$\gamma = 4\sqrt{\frac{2}{3}}C_1C_3 + \sqrt{2}C_2C_3 + \sqrt{10}C_2C_4. \quad (12)$$

The equation for g_0 corresponds to the one for the ground Γ_7 state of $5f^1$ electron in an octahedral symmetry. For g_{\perp} , we get the similar equation,

$$g_{\perp} = g_0 - \gamma. \quad (13)$$

As predicted, the g -value becomes anisotropic when the crystal field around a uranium ion is tetragonally distorted. The g -values for NpF_6 and Cs_2PaCl_6 were empirically determined to be negative (22, 23). The g -value for the isoelectronic U^{5+} is assumed to be negative. The average g -value, \bar{g} , will be calculated as follows:

$$\bar{g} = -\sqrt{\frac{1}{3}g_{||}^2 + \frac{2}{3}g_{\perp}^2}. \quad (14)$$

Figure 5 shows the variation of $g_{||}$, g_{\perp} , where

and \bar{g} -values with the tetragonal distortion parameter τ . With increasing τ , the anisotropy of the g -value becomes large. The average g -value, \bar{g} , decreases with increasing τ . For small tetragonal distortion ($\tau < 150 \text{ cm}^{-1}$), the change in \bar{g} is small. For $\tau = 100 \text{ cm}^{-1}$, $g_{||} = -0.468$, $g_{\perp} = -0.566$, and $\bar{g} = -0.473$ are obtained. This figure shows that the average g -value does not exceed -0.8 even for a very large tetragonal distortion (for example, $\tau = 1000 \text{ cm}^{-1}$). Even if covalency effects were considered, it is easily shown that this will simply increase the g -value (24). Therefore, we consider that the EPR spectrum with $g = 2.35$ – 2.50 for pure Li_3UO_4 (10) is attributable not to the $5f$ electron perturbed by an octahedral ligand field with/without tetragonal distortion, but to magnetic interaction of the $5f$ electron. In fact, Miyake *et al.* found magnetic interactions in MUO_3 ($M = \text{Li, Na, K, and Rb}$) which have distorted perovskite structures and measured EPR spectra with large g -values (25, 26).

The magnetic susceptibility of the molecule is given by the equation

$$\chi = \frac{N \sum_{n,m} [(E_{n,m}^{(1)})^2/kT - 2E_{n,m}^{(2)}] \exp(-E_{n,m}^0/kT)}{\sum_{n,m} \exp(-E_{n,m}^0/kT)}, \quad (15)$$

where N is the Avogadro's number, $E_{n,m}^0$ is the zero-field energy, $E_{n,m}^{(1)}$ and $E_{n,m}^{(2)}$ are the first- and second-order Zeeman terms, and n and m are quantum numbers. If the separation of levels within the ground state is much smaller than and the energy of the next excited state is much larger than kT , the susceptibility is expressed by the form (27)

$$\chi = \frac{Ng^2\beta^2}{4kT} + \text{TIP}, \quad (16)$$

$$g = 2\langle\Gamma_7|L + 2S|\Gamma_7\rangle$$

$$TIP = 2N\beta^2 \sum_i \frac{|\langle\Gamma_i|L + 2S|\Gamma_7\rangle|^2}{E(\Gamma_i) - E(\Gamma_7)}. \quad (17)$$

As a result of the tetragonal distortion, the magnetic susceptibility is anisotropic, i.e., both g and TIP are anisotropic. Since we have already obtained the wavefunctions for the ground doublets and excited states, the magnetic susceptibility of Li_3UO_4 is easily calculated by Eq. (16) as follows:

$$\begin{aligned} \chi &= \frac{1}{3}(\chi_{\parallel} + \chi_{\perp}) \\ &= 0.0210/T + 280 \times 10^{-6}. \end{aligned} \quad (18)$$

Our susceptibility data show good agreement with those calculated (Fig. 2). The discrepancy between the experimental results and calculated results at lower temperatures is due to magnetic interactions between uranium ions, which results in the large field dependence of the magnetic susceptibility below 7 K. This is observed by many research groups (6, 9, 10).

References

1. J. C. EISENSTEIN AND M. H. L. PRYCE, *Proc. R. Soc. London Ser. A* **255**, 181 (1960).
2. C. J. BALLHAUSEN, *Theor. Chim. Acta* **24**, 234 (1972).
3. H. G. HECHT, W. B. LEWIS, AND M. P. EASTMAN, *Adv. Chem. Phys.* **21**, 351 (1971).
4. N. EDELSTEIN, *Rev. Chim. Miner.* **14**, 149 (1977).
5. J. SELBIN, C. J. BALLHAUSEN, AND D. G. DURRETT, *Inorg. Chem.* **11**, 510 (1972).
6. B. KANELAKOPULOS, E. HENRICH, C. KELLER, F. BAUMGÄRTNER, E. KÖNIG, AND V. P. DESAI, *Chem. Phys.* **53**, 197 (1980).
7. G. BLASSE, *Z. Anorg. Allg. Chem.* **331**, 44 (1964).
8. S. KEMMLER-SACK, E. STUMPP, W. RÜDORFF, AND H. ERFURTH, *Z. Anorg. Allg. Chem.* **292**, 287 (1967).
9. C. KELLER, in "MTP International Review of Science," Vol. 7, "Lanthanides and Actinides" (K. W. Bagnall, Ed.), Series I, p. 47, Butterworths, London (1972).
10. C. MIYAKE, H. TAKEUCHI, H. OHYA-NISHIGUCHI, AND S. IMOTO, *Phys. Status Solidi A* **74**, 173 (1982).
11. W. B. LEWIS, H. G. HECHT, AND M. P. EASTMAN, *Inorg. Chem.* **12**, 1634 (1973).
12. S. R. DHARWADKAR AND M. S. CHANDRASEKHAR-AIAH, *Anal. Chim. Acta* **45**, 545 (1969).
13. T. FUJINO AND T. YAMASHITA, *Fresenius' Z. Anal. Chem.* **314**, 156 (1983).
14. L. L. SPARKS AND R. L. POWELL, *J. Res. Nat. Bur. Stand. Sect. A* **76**, 263 (1972).
15. Y. HINATSU AND T. FUJINO, *J. Solid State Chem.* **60**, 195 (1985).
16. B. R. JUDD, "Operator Techniques in Atomic Spectroscopy," McGraw-Hill, New York (1963).
17. "Gmelin Handbook of Inorganic Chemistry," Uranium, Supplement Volume A6, Springer-Verlag, New York/Berlin (1983).
18. P. RIGNY AND P. PLURIEN, *J. Phys. Chem. Solids* **28**, 2589 (1967).
19. S. KEMMLER-SACK, *Z. Anorg. Allg. Chem.* **363**, 295 (1968).
20. J. SELBIN AND H. J. SHERRILL, *Inorg. Chem.* **13**, 1235 (1974).
21. J. SELBIN AND J. D. ORTEGO, *Chem. Rev.* **69**, 657 (1969).
22. C. A. HUTCHISON, JR., AND B. WEINSTOCK, *J. Chem. Phys.* **32**, 56 (1960).
23. J. D. AXE, M. J. STAPLETON, C. D. JEFFERIES, *Phys. Rev.* **121**, 1630 (1961).
24. Y. HINATSU, T. FUJINO, AND N. EDELSTEIN, *J. Solid State Chem.*, in press (1992).
25. C. MIYAKE, K. FUJI, AND S. IMOTO, *Chem. Phys. Lett.* **46**, 349 (1977).
26. C. MIYAKE, K. FUJI, AND S. IMOTO, *Chem. Phys. Lett.* **61**, 124 (1979).
27. J. H. VAN VLECK, "The Theory of Electronic and Magnetic Susceptibilities," Oxford Univ. Press, London (1932).